

Vision Research (2021 online, 2022 printed)

Title: Cross-fixation interactions of orientations suggest high-to-low-level decoding in visual working memory

Authors: Long Luu<sup>1</sup>, Mingsha Zhang<sup>2</sup>, Misha Tsodyks<sup>3</sup> and Ning Qian<sup>1</sup>

Affiliation: <sup>1</sup>Department of Neuroscience, Zuckerman Institute, and  
Department of Physiology & Cellular Biophysics  
Columbia University  
New York, NY 10027

<sup>2</sup>State Key Laboratory of Cognitive Neuroscience and Learning  
IDG/McGovern Institute for Brain Research  
Beijing Normal University  
Beijing, 100875, China

<sup>3</sup>Simons Center for Systems Biology  
School of Natural Sciences  
Institute for Advanced Study  
Princeton, NJ 08540

Short title: Cross-fixation interactions of orientations

Keywords: visual decoding, perceptual bias, memory noise, retrospective Bayesian

Correspondence: Dr. Ning Qian  
3227 Broadway, JLG Rm L5-025  
New York, NY, 10027  
U.S.A.

nq6@columbia.edu  
Phone: 212-853-1105

# Cross-fixation interactions of orientations suggest high-to-low-level decoding in visual working memory

Long Luu, Mingsha Zhang, Misha Tsodyks and Ning Qian

## Abstract

1 Sensory encoding (how stimuli evoke sensory responses) is known to progress from low- to high-  
2 level features. Decoding (how responses lead to perception) is less understood but is often as-  
3 sumed to follow the same hierarchy. Accordingly, orientation decoding must occur in low-level ar-  
4 eas such as V1, without cross-fixation interactions. However, Ding et al (2017) provided evidence  
5 against the assumption and proposed that visual decoding may often follow a high-to-low-level hi-  
6 erarchy in working memory, where higher-to-lower-level constraints introduce interactions among  
7 lower-level features. If two orientations on opposite sides of the fixation are both task relevant and  
8 enter working memory, then they should interact with each other. We indeed found the predicted  
9 cross-fixation interactions (repulsion and correlation) between orientations. Control experiments  
10 and analyses ruled out alternative explanations such as reporting bias and adaptation across trials  
11 on the same side of the fixation. Moreover, we explained the data using Ding et al's retrospective  
12 high-to-low-level Bayesian decoding framework.

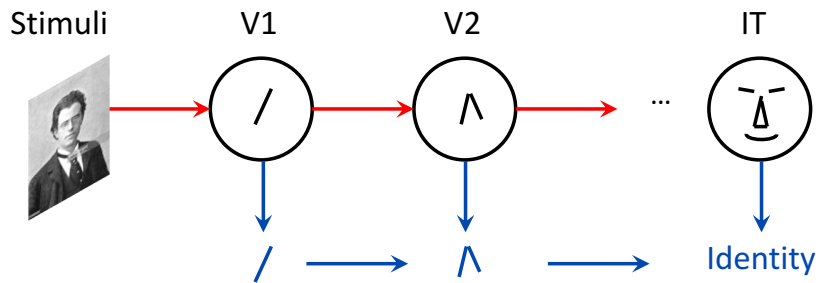
13 **Introduction**

14 Sensory processing can be framed as involving encoding and decoding (Seriès et al., 2009;  
15 Zhaoping, 2014). Encoding reflects how stimuli evoke responses in sensory neurons whereas  
16 decoding specifies how the responses eventually lead to perceptual judgments of the stimuli. A  
17 large body of research has established beyond doubt that visual encoding progresses from low to  
18 high levels, with neurons in later stages of a pathway responding to higher-level features (Felleman  
19 and Van, 1991; DiCarlo et al., 2012; Yamins and DiCarlo, 2016; Yamins et al., 2014; Riesenhuber  
20 and Poggio, 1999; Serre et al., 2007; Cichy et al., 2016). Decoding, however, is less understood  
21 because one has to rely on a decoding model to relate sensory responses to subjective perception.  
22 Many decoding models assume, sometimes implicitly, that decoding follows the same low-to-high-  
23 level hierarchy of encoding (exceptions discussed below). For example, to discriminate between  
24 two line orientations, one first decodes the absolute orientation of each line (a lower-level feature)  
25 and then compare the two absolute orientations to determine their relationship (a higher-level fea-  
26 ture) (Green et al., 1966; Paradiso, 1988; Seung and Sompolinsky, 1993; Graf et al., 2011; Teich  
27 and Qian, 2003). These models essentially assume that sensory responses generate perception  
28 (decoding) at about the same time the responses are evoked by stimuli (encoding) so that the  
29 decoding and encoding hierarchies are identical (Fig. 1a).

30 However, Ding et al. (2017) argued that perceptual decoding may often occur after initial sensory  
31 responses have entered working memory. This is likely whenever there is a delay between stim-  
32 ulus disappearance and perceptual judgment. Even under natural viewing conditions, because of  
33 our small fovea and frequent saccades, visual decoding may happen in working memory where  
34 patches of a scene from previous fixations are stored. Although the initial sensory responses to  
35 stimulus features (encoding) follow the low-to-high-level hierarchy, once all the relevant features  
36 are stored in working memory, their decoding, in principle, could be in any order. By considering  
37 invariance, noise tolerance, and behavioral relevance of high- vs. low-level features, Ding et al.  
38 (2017) proposed that sensory decoding in working memory should follow a high-to-low-level hi-  
39 erarchy, with the higher-level features producing a prior to constrain the decoding of lower-level  
40 features (retrospective Bayesian decoding, Fig. 1b). In particular, higher-level features are more  
41 categorical and thus can be stored in noise-resistant point attractors of working memory (Hopfield,  
42 1984). In contrast, lower-level features are more continuous and have to be stored in continuous  
43 attractors which are more prone to noise corruption over time (Compte et al., 2000; Itskov et al.,  
44 2011). It is therefore advantageous to decode more reliable higher-level features first and use  
45 them to constrain the decoding of less reliable lower-level features in noisy working memory.

46 To test these ideas, Ding et al. (2017) conducted an experiment in which two lines were flashed  
47 successively and then subjects reported the absolute orientations of both lines and (implicitly)

### a. Low-to-high-level decoding hierarchy



### b. High-to-low-level decoding hierarchy

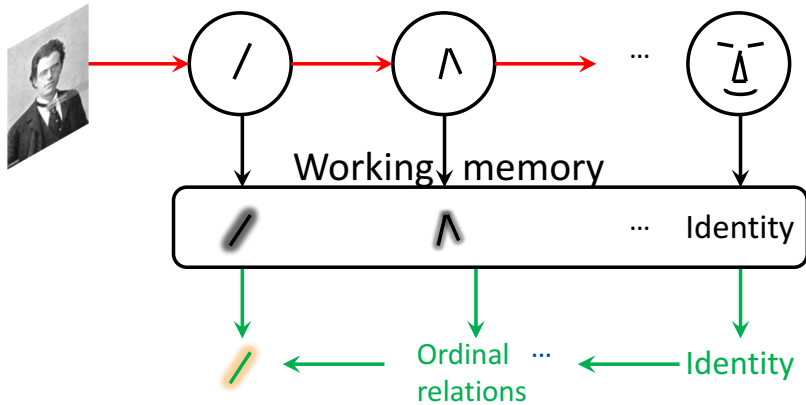


Figure 1: *Opposite decoding hierarchies*. In both panels, the red arrows indicate the well-established encoding hierarchy from low- to high-level features. (a) Low-to-high-level decoding of sensory responses (blue arrows). If encoding and decoding occur in sensory neurons at about the same time, then they must follow the same low-to-high-level hierarchy along sensory pathways. (b) High-to-low-level decoding in working memory (green arrows). If decoding happens after relevant features enter working memory, then it should progress from high to low levels, with higher-level features constraining lower-level features, because higher-level features are more invariant, reliable, and behaviorally relevant (Ding et al., 2017).

48 their ordinal relationship (whether the second line is clockwise or counter-clockwise from the first).  
49 They found that the two lines interacted perceptually in various ways that can be explained by  
50 the high-to-low-level decoding but not by the low-to-high-level decoding. For example, the second  
51 line repelled the first line (backward aftereffect) as much as the first line repelled the second  
52 line (forward aftereffect). The low-to-high-level decoding cannot explain the backward aftereffect  
53 because when the first line was decoded directly from its initial sensory response, the second  
54 line had not yet appeared. In contrast, the high-to-low-level decoding is assumed to occur after  
55 the encoding of both lines and their relationship have entered working memory where the higher-  
56 level ordinal relationship is decoded first, and then constrains the decoding of the lower-level  
57 absolute orientations to produce the observed mutual repulsion. The same mechanism accounts  
58 for another interaction: the correlation between two reported absolute orientations in a trial.

59 A surprising prediction of the high-to-low-level decoding scheme is that two stimuli traditionally  
60 considered as independent may interact with each other if they are both task relevant and repre-  
61 sented in working memory. A specific example is two orientation stimuli, or two translation-motion  
62 stimuli, on opposite sides of the fixation. Orientation or translation-motion interactions (such as  
63 adaptation aftereffects and simultaneous contrasts) typically require that the stimuli occupy the  
64 same or nearby regions on retina (Gibson and Radner, 1937; Meng et al., 2006; Xu et al., 2008).  
65 The standard explanation is that these simple features are first decoded in low-level areas such  
66 as V1 whose small receptive fields do not include both hemifields to support cross-fixation inter-  
67 actions. However, in such studies, usually only one stimulus, but not the other, is task relevant and  
68 stored in working memory. For example, in a standard adaptation paradigm, subjects only report  
69 the test stimulus, but not the adaptor. Similarly, the rod-and-frame illusion is usually demonstrated  
70 with the frame around the rod, instead of with the frame and rod on opposite sides of fixation, and  
71 subjects only report the rod, not the frame (Beh et al., 1971). We thus tested whether two lines  
72 could interact cross fixation when *both* lines were task relevant, and indeed found the predicted  
73 interactions. Moreover, we found the interactions regardless of whether subjects reported the two  
74 lines' orientations one after another continuously or with an interruption between the reports. Fi-  
75 nally, we demonstrated that Ding et al. (2017)'s high-to-low-level decoding framework explained  
76 the data from both reporting methods.

77 We note that a wealth of psychophysical results can be re-interpreted as high-to-low-level de-  
78 coding in working memory although the studies' original interpretations of formally similar models  
79 may be different (Luu and Stocker, 2018; Stocker and Simoncelli, 2008; Qiu et al., 2020; Fritzsche  
80 and de Lange, 2019; Jazayeri and Movshon, 2007; Zamboni et al., 2016; Bronfman et al., 2015;  
81 Talluri et al., 2018; Bae and Luck, 2017; Li et al., 2019) (see Ding et al. (2017) for detailed discus-  
82 sions). Another set of studies emphasize high-to-low-level processing (Navon, 1977; Chen, 1982;  
83 Ahissar and Hochstein, 2004; Oliva and Torralba, 2006) but they do not separate encoding and de-

84 coding hierarchies, or consider noisy working memory, or model how higher-level decoding affects  
85 lower-level decoding. There are also theories proposing bi-directional interactions along process-  
86 ing pathways (Atkinson and Shiffrin, 1968; Carpenter and Grossberg, 1987; Ullman, 1995; Lee  
87 and Mumford, 2003). While these theories address other important issues (such as the ART's so-  
88 lution to the stability-plasticity dilemma), they are not concerned with how noise in working memory  
89 may shape the decoding hierarchy (Ding et al., 2017). To our knowledge, previous studies never  
90 predicted nor tested cross-fixation interactions of remembered orientations. We therefore believe  
91 that by distinguishing between the encoding and decoding hierarchies and specifying the decod-  
92 ing mechanisms as high-to-low-level constraints in working memory, the retrospective Bayesian  
93 scheme (Ding et al., 2017) may provide a coherent framework for understanding a range of per-  
94 ceptual phenomena. Preliminary results were published in abstract form (Luu et al., 2020).

## 95 **Methods**

### 96 **Experimental procedure**

97 Fifteen subjects with normal or corrected-to-normal vision (10 males, 5 females; all naïve) partici-  
98 pated in the experiments. All subjects provided informed consent. The experiments were approved  
99 by the Institutional Review Board of Columbia University.

100 *General procedure:* During the experiments, subjects sat in a darkened room and viewed the  
101 stimuli on a large-screen monitor (Samsung QN55Q6F, 55 inch, refresh rate: 120 Hz and reso-  
102 lution: 3840 x 2160 pixels) at a distance of 56 cm. We enforced the viewing distance and head  
103 stabilization with a chin rest and head band. All experiments were run in Matlab (Mathworks,  
104 Inc.) in combination with PsychoPhysics Toolbox (Brainard, 1997). A Dell computer (Intel core i7-  
105 8700, 16GB RAM and NVidia GTX 1060 graphics card) controlled the stimulus presentation, and  
106 another Dell computer (i5-8400, 8GB RAM) controlled an infrared video-based eye tracker devel-  
107 oped in Mingsha Zhang's lab (1000 Hz sampling rate). Subjects' gaze were always monitored  
108 during the experiment. There were three experimental conditions run in separate blocks. Before  
109 each condition, we gave subjects detailed instruction on the task and let them practice until they  
110 were comfortable with their performance. Each stimulus line was  $6^\circ$  by  $0.1^\circ$ .

111 *1-line condition:* At the beginning of a trial, subjects had to maintain fixation on a white dot  
112 (diameter:  $0.27^\circ$ ) at the center of the screen. The trial only started when subjects successfully  
113 maintained fixation within a circular window (radius:  $3^\circ$ ) around the fixation dot for 1 second.  
114 A line then appeared on either the left or right side (counter-balanced and randomized) of the  
115 fixation dot, centered at the eccentricity of  $8^\circ$ . The line color was magenta and green for the left

116 and right side, respectively. The line's orientation was either 49° or 54° from the horizontal in two  
117 separate blocks. During the presentation, if subjects' gaze broke the fixation window, a tone (200  
118 Hz, 0.5 second) was played, and the trial was aborted and repeated. After a 1-second duration,  
119 the stimulus line disappeared and a beep (400 Hz, 0.2 second) was played to prompt subjects to  
120 report the orientation of the stimulus line. To report the line's orientation, subjects first moved the  
121 mouse along the perceived orientation. After the mouse motion started, a marker line appeared at  
122 the fixation with an orientation along the mouse's moving direction. The marker line had the same  
123 color and length as the stimulus line. Subjects then rotated the marker line with the mouse to  
124 fine-tune their estimate of the stimulus orientation, and left-clicked to report. They were instructed  
125 to take time to be as accurate as possible.

126 *2-line condition:* Similar to the 1-line condition, subjects had to successfully maintain fixation for  
127 1 sec before the stimulus presentation. Then, two colored lines were presented on the opposite  
128 sides of the fixation dot, each centered at the eccentricity of 8°. Consistent with the 1-line con-  
129 dition, the left line was magenta and the right line was green. The lines' orientations were 49°  
130 and 54° that were counter-balanced and randomized across trials. As for the 1-line condition, a  
131 trial was aborted and repeated whenever subjects broke the fixation window during the stimulus  
132 presentation. This ensured that the two stimulus lines always occupied well-separated retinal lo-  
133 cations on opposite sides of the fixation. After 1 second, the stimulus lines disappeared and a tone  
134 prompted subjects to first report the orientation of the left line by drawing and adjusting a magenta  
135 marker line. After subjects clicked to confirm the estimate of the left line orientation, the marker  
136 line changed color from magenta to green and subjects rotated it to the estimate of the right line  
137 orientation and clicked again. Note that subjects always reported the left line first and then the  
138 right line, to avoid any potential confusion.

139 *2-line-interrupt condition:* The experimental procedure was identical to that for the 2-line con-  
140 dition except that after subjects clicked to confirm the report of left line, the magenta marker line  
141 disappeared, and subjects had to move the mouse again to draw the green marker line and used  
142 it to report the right line's orientation.

## 143 Data analysis

144 *Computation and statistical test of repulsion and correlation:* To compute the repulsion and cor-  
145 relation of subjects' reports of the two lines, we first flipped (mirrored) all the incorrect trials with  
146 respect to the diagonal line (see Results for explanations). Then we computed the mean differ-  
147 ence and Pearson correlation between the two reports in a trial. The repulsion was computed  
148 by subtracting the mean difference of the baseline, 1-line condition from that of the 2-line or 2-  
149 line-interrupt conditions. To test the significance of the observed effects at the group level, we

150 first obtained the mean values of repulsion and correlation for each individual subject. Then we  
151 use Wilcoxon sign rank test on these values. For the statistical test of individual subjects, we  
152 used bootstrapping ( $n = 10,000$ ) to obtain the 95% confidence interval of the mean difference and  
153 correlation for each subject. Then we plot the results of the 2-line or 2-line-interrupt conditions  
154 versus the 1-line condition. If the confidence interval did not touch the diagonal line, the effect was  
155 statistically significant at 0.05 level.

156 *Analysis of cross-trial adaptation at the same site:* We quantified how much traditional adap-  
157 tation across trials on the same site contributed to the observed repulsion effect in the 2-line  
158 condition. In the separate  $n$ -back analysis, we split the trials into the "same" and "different" sets  
159 according to whether stimulus orientations of a given trial and the  $n$ -back trial were the same or  
160 different. In the cumulative  $n$ -back analysis, we split the trials into the "same" and "different" sets  
161 according to whether stimulus orientations of a given trial and all the  $n$  previous trials were the  
162 same or different. This required the  $n$  previous trials all had the same orientation, thus halving  
163 the number of available data points with each increment of  $n$ . For each set, we computed the  
164 repulsion by subtracting the mean difference in the 1-line condition from the mean difference in  
165 the 2-line condition. To measure how much the traditional adaptation contributed to the observed  
166 repulsion, we used the adaptation index:  $(R_d - R_s)/(R_d + R_s)$ , where  $R_d$  and  $R_s$  are the repulsion  
167 of the "different" and "same" sets, respectively.

## 168 Decoding models

### 169 Model descriptions

170 *The 1-line condition:* We assume that the two orientations are represented independently, each  
171 with Gaussian sensory and memory noises, and decoded independently. When stimulus orien-  
172 tation  $\theta_i, i = 1, 2$  is presented in a trial, a sensory sample  $s_i$  is drawn according to the Gaussian  
173 probability density  $p(S_i|\theta_i) = N(\theta_i, \sigma_s)$ . Then at the report time, a memory sample  $m_i$  is drawn  
174 according to the Gaussian probability density  $p(M_i|s_i) = N(s_i, \sigma_m)$ . A Bayesian decoder with a  
175 uniform prior generates an estimate of the stimulus orientation at the center-of-mass of the likeli-  
176 hood function, which in this case equals the memory sample  $m_i$ .

177 *The 2-line condition with low-to-high-level decoding:* According to the low-to-high-level decoding  
178 scheme, the two (lower-level) absolute orientations in a 2-line trial are first decoded independently  
179 (as in the 1-line case), and the results are then compared to decode the (higher-level) relationship  
180 between the orientations. Thus, according to this scheme, the 1-line data predicts the 2-line data.  
181 Specifically, for the low-to-high-level decoding, we sampled from the measured 1-line distributions  
182 of the two orientations to generate the predicted 2-line joint distribution and its derived proper-

ties (difference distribution, correlation, and repulsion). Note that the low-to-high-level decoding model does not involve working memory (Fig. 1a) but the 1-line data must contain both sensory and memory noise. However, there is no need to separate the noise sources since this model predicts the 2-line data poorly regardless of the noise level: the model cannot explain the cross-fixation interactions (correlation and repulsion) in the 2-line data because it treats the two absolute orientations separately.

*The 2-line condition with high-to-low decoding:* The model makes the same assumptions about the sensory and memory noise as for the 1-line case to produce a likelihood function for the absolute orientations:  $p(m_1, m_2|\theta_1, \theta_2) = p(m_1|\theta_1)p(m_2|\theta_2)$  except that we used a different  $\sigma_m$  for the memory noise because subjects had to memorize two lines instead of one. The decoding procedure (Ding et al., 2017), however, follows the opposite hierarchy of the low-to-high-level scheme above. First, the model uses the sensory sample  $s_1$  and  $s_2$  of the left and right orientations in a trial to decode their ordinal relationship  $\hat{O}$ , namely whether the left orientation is larger or smaller than the right orientation. Formally,  $\hat{O}$  is the option that maximizes the posterior for the ordinal choice  $O$  given the sensory samples,  $p(O|s_1, s_2)$ . Since a priori the two options were equally probable in our experiments, we determine  $\hat{O}$  according to whether  $s_1$  is larger or smaller than  $s_2$ .

Since the discrete choice  $\hat{O}$  can be stored in a noise-resistant, point attractor of the memory system, we assume it is immune to the memory noise (Ding et al., 2017). In contrast, the sensory sample  $s_1$  and  $s_2$  for the continuous, absolute orientations have to be stored in continuous, ring attractors which are prone to memory noise, and at the report time, they become memory samples  $m_1$  and  $m_2$  in a trial. If the ordinal decoding  $\hat{O}$  is usually correct, then using it to constrain the likelihood function of  $m_1$  and  $m_2$  can improve the accuracy of the absolute decoding. Specifically,  $\hat{O}$  produces a prior,  $p(\theta_1, \theta_2|\hat{O})$ , which is a step function along the diagonal line in the joint space of the two orientations. The opposite choices of  $\hat{O}$  produce the corresponding, opposite step functions. Multiplying this prior to the likelihood function produces the posterior of the absolute orientations:

$$p(\theta_1, \theta_2|m_1, m_2, \hat{O}) \propto p(m_1, m_2|\theta_1, \theta_2) p(\theta_1, \theta_2|\hat{O}) \quad (1)$$

The prior erases the part of the likelihood function either above or below the diagonal line that is inconsistent with the ordinal judgment  $\hat{O}$ . Then the stimulus absolute orientations are decoded as the mean of their posterior:

$$\hat{\theta}_i = \iint \theta_i p(\theta_1, \theta_2|m_1, m_2, \hat{O}) d\theta_1 d\theta_2 \quad (2)$$

for  $i = 1, 2$ .

*The 2-line-interrupt condition with high-to-low decoding:* The model is identical to the high-to-low decoding model for the 2-line condition up to the posterior  $p(\theta_1, \theta_2|m_1, m_2, \hat{O})$ . However, only the

216 left orientation decoded from the posterior is reported before the interruption (the disappearance  
 217 of the marker line). After the interruption, we assume that the process of redrawing the marker  
 218 line again for the second report means that a new memory sample  $(m'_1, m'_2)$  is drawn to form a  
 219 new posterior,  $p(\theta_1, \theta_2 | m'_1, m'_2, \hat{O})$ , in the same way as we did for  $p(\theta_1, \theta_2 | m_1, m_2, \hat{O})$ . This time  
 220 only the right orientation decoded from the new posterior is reported. We considered two ways  
 221 for drawing the new memory sample, producing two versions of the model. The first version is to  
 222 draw  $m'_i$  from the Gaussian density  $N(m_i, \sigma_m)$ ; this means that the new memory sample is the  
 223 old memory sample further corrupted by memory noise. The second version is to draw  $m'_i$  from  
 224 the Gaussian density  $N(\hat{\theta}_i, \sigma_m)$  where  $\hat{\theta}_i$  are the estimate of the first decoding. This means that  
 225 the new memory sample is the first decoded orientations further corrupted by memory noise. In  
 226 both versions, we assume that the new noise has the same  $\sigma_m$  as the memory noise for the first  
 227 decoding. We believe this is a good approximation because the reaction times of the first and  
 228 second reports are similar in the 2-line-interrupt condition (see Supplementary Fig. S4b).

229 **Model fitting procedures**

230 To fit the models to subjects' data, we first obtain the distribution of the decoded orientations  
 231 given the actual orientations,  $p(\hat{\theta}_1, \hat{\theta}_2 | \theta_1, \theta_2)$ , by marginalizing (integrating over) the latent memory  
 232 variables and the ordinal judgment variable:

$$p(\hat{\theta}_1, \hat{\theta}_2 | \theta_1, \theta_2) = \sum_{\hat{O}} p(\hat{O} | \theta_1, \theta_2) \iint p(\hat{\theta}_1, \hat{\theta}_2 | m_1, m_2, \hat{O}) p(m_1, m_2 | \theta_1, \theta_2) dm_1 dm_2. \quad (3)$$

233 For Gaussian noises, this can also be done with Ding et al. (2017)'s analytical formula (their Eqs. 1  
 234 and 2) for  $\hat{\theta}_1$  and  $\hat{\theta}_2$  by sampling  $m_1$ ,  $m_2$ , and  $\hat{O}$  for given  $\theta_1$  and  $\theta_2$ . (Note that  $m_i$  was called  $r_i$ , and  
 235  $\sigma_s^2 + \sigma_m^2 = \sigma_i^2$  in Eqs. 1 and 2 of Ding et al. (2017), and the two opposite choices of  $\hat{O}$  correspond  
 236 to swapping  $\hat{\theta}_1$  and  $\hat{\theta}_2$  in the two equations.)

237 We then use  $p(\hat{\theta}_1, \hat{\theta}_2 | \theta_1, \theta_2)$  to obtain the difference distribution  $p(\hat{\theta}_2 - \hat{\theta}_1 | \theta_1, \theta_2)$ . We jointly fit the  
 238 model to the 1-line and 2-line data pooled over all subjects by maximizing the likelihood of data  
 239 with respect to the model parameters using Nelder-Mead algorithm. The model has 3 parameters:  
 240 the sensory noise  $\sigma_s$  and the separate memory noises  $\sigma_m$  for the 1-line and the 2-line conditions.  
 241 For the 2-line data, we fit the difference distribution instead of the joint distribution because the  
 242 joint distribution is 2D and we do not have a large amount of data to fit it robustly. Moreover,  
 243 fitting the difference distribution can already capture the characteristic bimodal pattern of the joint  
 244 distribution.

245 **Model prediction for the 2-line-interrupt condition**

246 Given the fit parameters for the 1-line and 2-line conditions, we predict the 2 line-interrupt condi-  
 247 tion without new free parameters using the two high-to-low-level decoding steps described above.

248 **Results**

249 **Cross-fixation interactions of orientations in working memory**

250 The first experiment was similar to that of Ding et al. (2017) but instead of presenting two lines  
251 sequentially at the fixation, we presented them simultaneously on opposite sides of the fixation  
252 point (Fig. 2b), for 1 sec. The lines were  $6^\circ$  by  $0.1^\circ$ , and oriented  $49^\circ$  and  $54^\circ$  from horizontal, re-  
253 spectively. The two orientations were counter-balanced and randomized for the two sides over 50  
254 trials of a block. The center-to-center distance between the lines was  $16^\circ$ . An infrared eye tracker  
255 (see Methods) was employed to monitor eye position online, and each trial started after subjects  
256 acquired fixation for 1 sec. The fixation window was a circle of  $3^\circ$  radius, and trials with broken  
257 fixation during stimulus presentation were aborted and repeated. After the lines disappeared, sub-  
258 jects first reported the left line's orientation by drawing a marker line with a mouse according to the  
259 perceived orientation, adjusting it to match the perceived orientation as closely as possible, and  
260 clicking a button. They then continued to rotate the marker line to match the right line's orientation  
261 as closely as possible and clicked to report. As in Ding et al. (2017), the continuation from the  
262 first to the second report let subjects implicitly indicate the lines' ordinal relationship (the second  
263 experiment below interrupted this continuation). After an inter-trial-interval of 300-600 ms, the next  
264 trial started. To minimize potential mix-up of the two stimulus lines, we always colored the left and  
265 right lines magenta and green, respectively, and changed the marker line color from magenta to  
266 green after the first click (Fig. 2b).

267 In addition to the above 2-line condition, we also ran the corresponding baseline, 1-line condi-  
268 tion, in which only one line (either  $49^\circ$  or  $54^\circ$  in separate 50-trial blocks) was presented either on  
269 the left or on the right of the fixation (counter-balanced and randomized) and subjects reported its  
270 orientation as they did for the first line in the 2-line condition (Fig. 2a).

271 We collected data from 15 subjects (all naive). We first describe the distributions of the re-  
272 ported absolute orientations of the individual lines. In the 1-line condition, the absolute distribu-  
273 tions (Fig. 2c) are roughly centered at the lines' actual orientations ( $49^\circ$  and  $54^\circ$ ). The difference  
274 between the means of the two distributions is  $5.3^\circ$ , close to the actual  $5^\circ$  difference. In the 2-line  
275 condition, the absolute distributions (Fig. 2d) for the two lines are further apart compared with  
276 those of the 1-line condition, with an  $8.6^\circ$  difference between the means, indicating a perceptual  
277 repulsion between the lines. The repulsion is statistically significant ( $p = 0.00006$ , Wilcoxon sign  
278 rank test).

279 There was considerable variability of the reported absolute orientations. Because the stimulus  
280 lines were flashed on the periphery and subjects reported well after the stimuli disappeared, the  
281 variability must reflect both sensory and memory noises. The variance of absolute distributions in

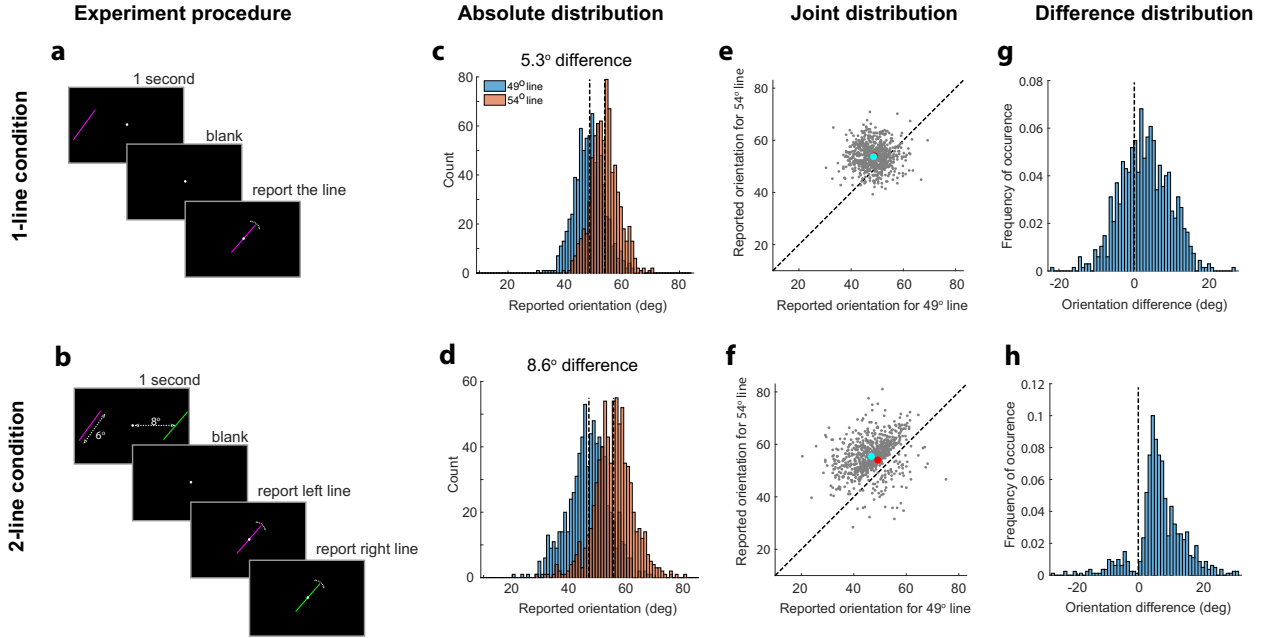


Figure 2: *The 1-line and 2-line conditions with data pooled from all 15 naive subjects.* (a) Trial sequence for the 1-line condition. (b) Trial sequence for the 2-line condition. For both conditions, during the blank after the stimulus disappearance, subjects drew a marker line for reporting. See text and Methods for details. (c, d) Reported distributions of the stimulus lines' absolute orientations for the 1-line and 2-line conditions, respectively. For each condition, the distributions for the  $49^\circ$  and  $54^\circ$  lines are in blue and orange, respectively. The dashed vertical lines indicate the means of the distributions. The difference between the means was greater in the 2-line condition than that in the 1-line condition, indicating repulsion. (e) Simulated joint distribution of the 2-line condition predicted from the 1-line data according to the low-to-high-level decoding scheme. (f) The measured joint distribution of the 2-line condition. The red dot indicates the true stimulus orientations, and the cyan dot indicates the means of the reports. The measured distribution showed a correlation between the two reports in a trial and a bimodal pattern with shifts away from the diagonal line whereas the joint distribution predicted by the low-to-high-level decoding did not. (g-h) The difference distributions (the  $54^\circ$  line minus the  $49^\circ$  line), obtained from the simulated and measured joint distributions in panels e and f, respectively. They are equivalent to projecting the joint distributions along the negative diagonal axis.

282 the 2-line condition was also greater than that of the 1-line condition ( $p = 0.00006$ , Wilcoxon sign  
283 rank test, see Fig. S1). Since the stimulus orientations and duration were exactly the same for  
284 the two conditions, the greater variance in the 2-line condition was likely due to increased memory  
285 noise because subjects had to hold two lines in working memory instead of one line.

286 We next examined the joint distribution of the two reported orientations in a trial of the 2-line  
287 condition. Fig. 2f plots the report for the  $54^\circ$  line against that for the  $49^\circ$  line. The distribution was  
288 elongated along the diagonal, indicating a positive correlation between the two reports in a trial ( $p$   
289 =  $0.00006$ , Wilcoxon sign rank test). The data points above and below the diagonal line were from  
290 the trials with correct and incorrect ordinal judgments, respectively. There was a gap between  
291 these two sets of trials as they shifted away from the diagonal (the decision boundary for the  
292 ordinal judgments), rendering the joint distribution bimodal. By subtracting the  $49^\circ$  report from the  
293  $54^\circ$  report in a trial, we obtained the difference distribution (Fig. 2h), which was also bimodal. The  
294 difference distribution is equivalent to projecting the joint distribution along the negative diagonal  
295 axis, and the correct and incorrect trials are on the left and right sides of 0, respectively.

296 These results were quite similar to those of Ding et al. (2017). Importantly, Ding et al. presented  
297 the two lines successively at the same spatial location whereas here we presented them simul-  
298 taneously on opposite sides of the fixation. This suggests that the two lines interacted similarly  
299 in working memory regardless of whether they were presented at the same or very different loca-  
300 tions. Also similar to Ding et al.'s findings, the results of the 2-line condition cannot be explained  
301 by the low-to-high-level decoding scheme, which assumes that V1 cells in opposite hemispheres  
302 first decode the two lines' absolute orientations separately, which are then compared to determine  
303 their relationship. Obviously this decoding scheme cannot reproduce the observed interactions  
304 between the lines. We simulated this scheme's predicted joint distribution in Fig. 2e by randomly  
305 sampling pairs of orientations from the  $49^\circ$  and  $54^\circ$  distributions of the 1-line condition. This joint  
306 distribution is unimodal, and centered on, and evenly distributed around, the physical stimulus ori-  
307 entations, without the correlation, gap, and repulsion in the 2-line data. The predicted difference  
308 distribution is also unimodal, symmetrically centered on the actual difference between the two  
309 lines' orientations ( $5^\circ$ ), again unlike the measured difference distribution of the 2-line condition.

310 Although we pooled all subjects' data above, the interactions between the lines in the 2-line  
311 condition (repulsion and correlation) were consistently observed across all subjects (see Supple-  
312 mentary Fig. S2 for the joint distributions of all individual subjects). We computed each subject's  
313 repulsion and correlation in the 2-line condition, and compared with those predicted from the low-  
314 to-high-level decoding scheme applied to the 1-line data. Since the repulsion and correlation  
315 occurred separately for the correct and incorrect trials (trials above and below the diagonal line  
316 in Fig. 2f), we flipped (mirrored) the incorrect trials with respect to the diagonal line before the  
317 computation, and applied the same procedure to the simulated joint distributions from the 1-line

318 data. (Without the flipping, we would underestimate the repulsion and correlation, particularly for  
 319 subjects with a large number of incorrect trials, because the repulsion values in the two opposite  
 320 directions away from the diagonal would cancel each other, and the separation, along the nega-  
 321 tive diagonal, of the two positive-diagonal elongations would reduce the actual correlation.) Fig. 3a  
 322 shows that all 15 subjects reported greater orientation difference in the 2-line condition than in the  
 323 1-line condition. We computed the 95% confidence interval using bootstrapping for each subject,  
 324 and found that for 12 out of the 15 subjects, the 95% confidence interval did not touch the diag-  
 325 onal line in Fig. 3a. Therefore, the repulsion in the 2-line condition is significant for the majority  
 326 of subjects individually. Fig. 3b shows that the correlation in the 2-line condition was greater than  
 327 that in the 1-line condition. Again, the 95% confidence interval for each subject calculated with  
 328 bootstrapping indicates that 12 out of the 15 subjects showed significant correlation individually.

329 Finally, Fig. 3c shows that the ordinal discrimination performance in the 2-line condition was  
 330 better than that predicted by the 1-line data according to the low-to-high-level decoding (mean  
 331 accuracy: 90% vs. 77%). The difference is significant at the group level ( $p = 0.025$ , Wilcoxon  
 332 sign rank test). This can also be seen in the joint and difference distributions in Fig. 2 which  
 333 show a larger portion of correct trials in the 2-line condition compared to the 1-line condition. At  
 334 the individual level, 11 out of the 15 subjects showed the same trend (Fig. 3c) although only 5  
 335 subjects reached significance based on the bootstrapping test.

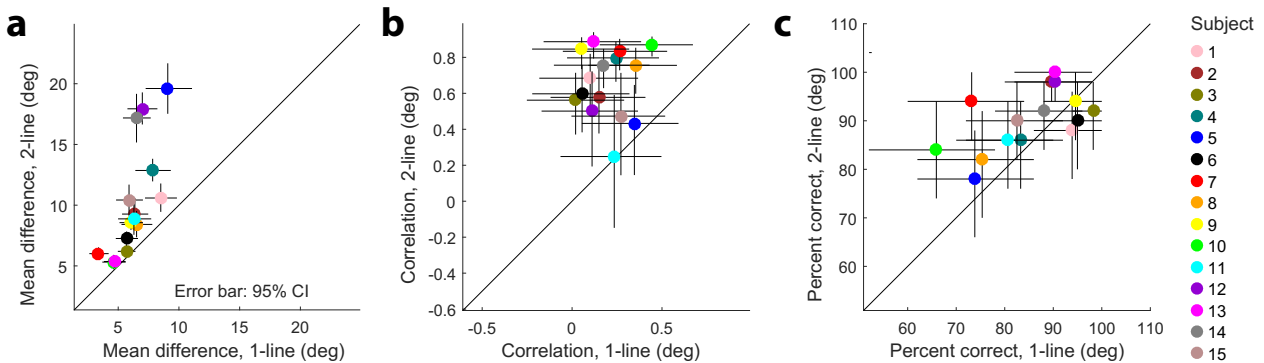


Figure 3: *Comparison of the 1-line and 2-line conditions for individual subjects.* Each color represents one subject. (a) The mean absolute difference between the reports for the 49° and 54° lines. (b) The correlation coefficient between the two reports in a trial. The correlation for the 1-line condition was based on the prediction of the low-to-high-level decoding. (c) The percentage correct of ordinal discrimination between the two lines. The percentage correct for the 1-line condition was based on the prediction of the low-to-high-level decoding. All error bars were 95% confidence intervals obtained by bootstrapping 10,000 times.

336 The above results suggest that when stimulus orientations are decoded in working memory,  
 337 they interact with each other even when presented on opposite sides of the fixation. However,

338 there are two potential confounds and we address them below.

339 **Orientation interactions under a different report method**

340 The first potential confound is that in the 2-line condition above, subjects rotated the marker line  
341 continuously from the first report to the second report, and this continuity might introduce interac-  
342 tions artificially. For example, subjects might over-rotate to ensure that the two reports were differ-  
343 ent even though the instructions emphasized accuracy. This, however, was unlikely because the  
344 actual  $5^\circ$  orientation difference was well above the orientation discrimination threshold of around  $1^\circ$   
345 at fovea where the marker line was placed. To directly address any potential problems of the con-  
346 tinuous report method above, we did a control experiment by running the same group of subjects  
347 on the 2-line condition with an interruption between the two reports (2-line-interrupt condition). It  
348 was identical to the above 2-line condition except that after subjects clicked to report the left ori-  
349 entation, the marker line immediately disappeared and subjects had to move the mouse to redraw  
350 the marker line according to their perceived right orientation, adjusted it to match the perception  
351 as closely as possible, and then clicked (Fig. 4a). This method was very similar to that used by  
352 Bae and Luck (2017) but they presented stimuli at fovea and did not measure cross-fixation inter-  
353 actions. We planned both reporting methods before the data collection and randomized the order  
354 of the 2-line and 2-line-interrupt conditions across subjects.

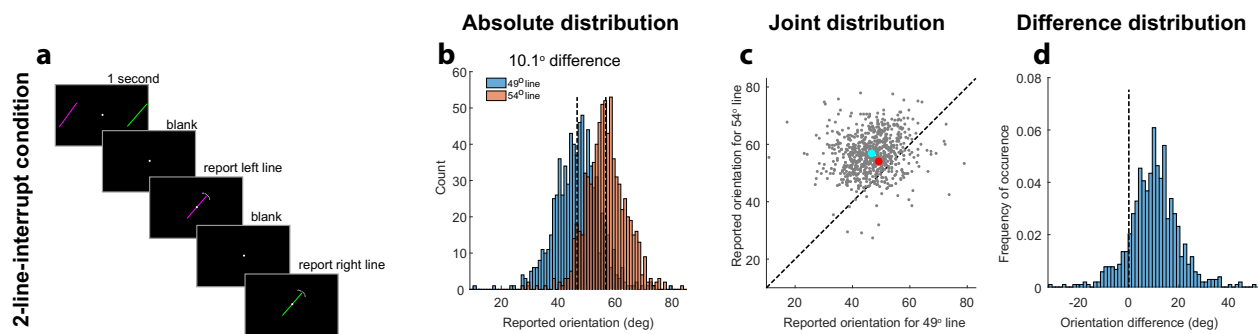


Figure 4: *The 2-line-interrupt condition with data pooled from all 15 naive subjects.* The plot format is identical to that of Fig. 2. (a) Trial sequence for the 2-line-interrupt condition. During each blank, subjects drew a marker line for reporting. The second blank interrupted the continuity of the two reports. See text and Methods for details. (b) Reported distributions of the stimulus lines' absolute orientations, showing even larger repulsion between the  $49^\circ$  and  $54^\circ$  lines than that for the 2-line condition (Fig. 2d). (c) The joint distribution, showing much reduced correlation and bimodality compared with the 2-line condition (Fig. 2f). (d) The distribution of the difference between the two reported orientations, again showing a much reduced bimodality compared with the 2-line condition (Fig. 2h).

355 The results pooled across all subjects are shown in Fig. 4. The distributions of the reported  
 356 absolute orientations (Fig. 4b) showed a significant repulsion compared with the 1-line condition  
 357 ( $p = 0.0003$ , Wilcoxon sign rank test). In fact, the repulsion in the 2-line-interrupt condition (mean  
 358 orientation difference  $10.1^\circ$ ) was even larger than that in the 2-line condition (mean orientation  
 359 difference  $8.6^\circ$ ). However, the interrupt report method changed the joint distribution of the two  
 360 reports in a trial (Fig. 4c). Although the joint distribution shifted away from the diagonal, there  
 361 was no clear gap between the correct and incorrect trials along the diagonal, and the difference  
 362 distribution was unimodal (Fig. 4d). The correlation between the two reports in a trial was much  
 363 reduced though still significant ( $p = 0.035$ , Wilcoxon sign rank test).

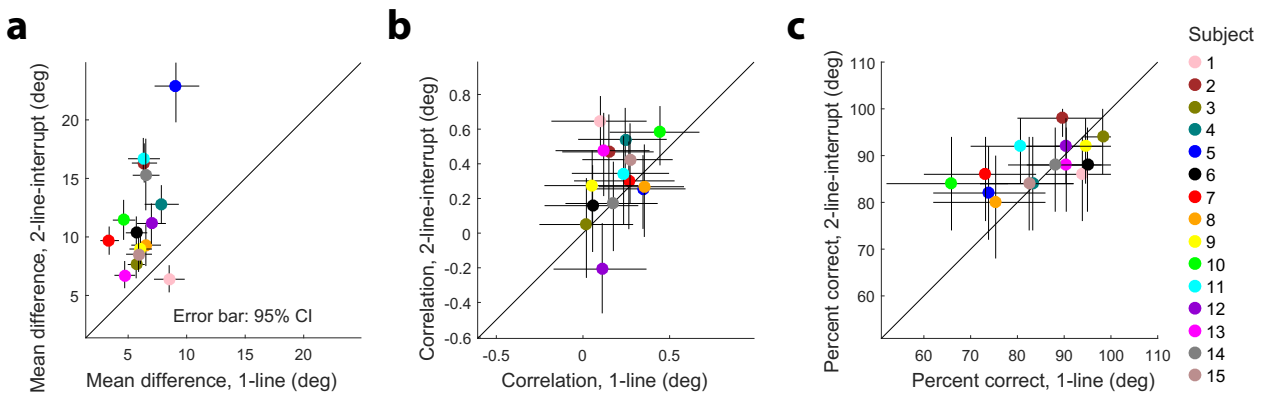


Figure 5: *Comparison of the 1-line and 2-line-interrupt conditions for individual subjects.* The plot format is identical to that of Fig. 3. **(a)** The mean absolute difference between the reports for the  $49^\circ$  and  $54^\circ$  lines. **(b)** The correlation coefficient between the two reports in a trial. The correlation for the 1-line condition is based on the prediction of the low-to-high-level decoding in Fig. 2e. **(c)** The percentage correct of ordinal discrimination between the two lines. Note that the subjects did not explicitly perform the ordinal discrimination task so the percent correct was inferred from their reported absolute orientations of the stimuli. All error bars were 95% confidence intervals obtained by bootstrapping 10,000 times.

364 We also analyzed the 2-line-interrupt data for each subject individually, as we did for the 2-line  
 365 condition. We found that 14 out of 15 subjects showed a significant repulsion (Fig. 5a), and the  
 366 repulsion magnitudes were generally greater than those for the 2-line condition (cf. Fig. 3a). The  
 367 correlations were weaker than those for the 2-line condition (cf. Figs. 5b and 3b). This can also be  
 368 seen from shapes of individual subjects' joint distributions of the 2-line-interrupt condition in Sup-  
 369 plementary Fig. S3. Although some subjects showed similar joint distributions for the two report  
 370 methods, others showed little elongation along the diagonal under the interrupted report method.  
 371 Finally, Fig. 5c shows the subjects' ordinal discrimination performances; unlike the original 2-line  
 372 condition, the mean was not significantly better than that predicted by the 1-line data ( $p = 0.23$ ).  
 373 This is perhaps not surprising because the interruption must make it difficult (and unnecessary) for

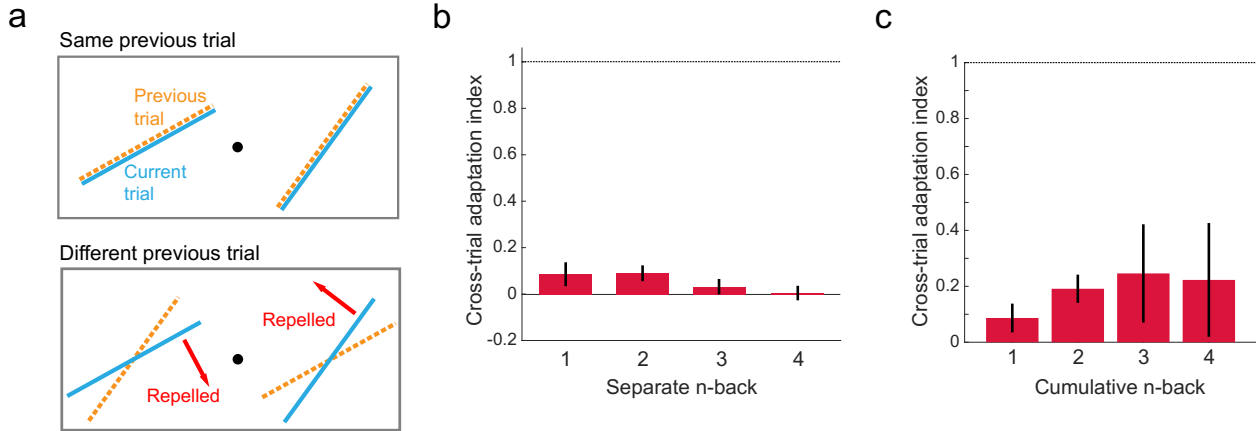


Figure 6: *Cross-trial adaptation at the same site cannot explain the observed repulsion* (a) The orientations of the current (blue) and a previous (yellow) trial can be either the same (top) or different (bottom). The "different" case could produce cross-trial adaptation aftereffect whereas the "same" case could not. (b)  $n$ -back cross-trial adaptation index for the 2-line condition, with  $n = 1, 2, 3$  and  $4$  separately. The index values of 0 and 1 indicate that cross-trial adaptation explains none and all of the measured repulsion, respectively. (c) Cumulative  $n$ -back cross-trial adaptation index for the 2-line condition, with  $n = 1, 2, 3$  and  $4$ . All error bars represent  $\pm 1$  SEM. They grow with  $n$  in panel c because the number of available data points is halved for each increment of cumulative  $n$ .

374 the subjects to indicate the ordinal relationship through the two absolute reports. In other words,  
 375 the ordinal discrimination performances calculated from the 2-line-interrupt data did not reflect the  
 376 subjects' actual ordinal discrimination performances.

377 In sum, interrupting the continuity of the two reports in a trial did not eliminate the cross-fixation  
 378 interactions of orientations. Both the repulsion and correlation remained significant at the group  
 379 level. Although the correlation was much weaker, the repulsion appeared stronger. We will explain  
 380 these data and their differences in a modeling section later.

381 **The repulsion cannot be explained by adaptation across trials at the same site**

382 Another potential confound of the 2-line condition is that the observed repulsion might be explained  
 383 by traditional adaptation aftereffects across trials on the same side of the fixation. Specifically, at  
 384 a given site, if the stimulus orientation in the current trial was different from that in a previous trial,  
 385 subjects' perceived orientation in the current trial could be repelled away from the orientation of  
 386 the previous trial (Fig. 6a). However, if the stimulus orientations for the two trials were identical,  
 387 then there would be no adaptation-induced repulsion (Gibson and Radner, 1937). We first note  
 388 that such cross-trial adaptation aftereffects must be small because of the long intervals between

389 stimuli of successive trials (around 8 sec for the 2-line condition) compared to the stimulus duration  
390 (1 sec). It might be further reduced by the attractive, serial effect (Fischer and Whitney, 2014).  
391 Nevertheless, we analyzed this possibility in great detail. First, we split each subject's 2-line data  
392 into the "same" and "different" sets according to whether the stimulus orientation in a trial and that  
393  $n$  trials back were identical or not, for  $n = 1, 2, 3$ , and 4. We quantified the  $n$ -back cross-trial  
394 adaptation effect by calculating the index  $(R_d - R_s)/(R_d + R_s)$ , where  $R_d$  and  $R_s$  are the repulsion  
395 of the "different" and "same" sets, respectively. If the repulsion all came from the  $n$ -back cross-  
396 trial adaptation, instead of from cross-fixation interactions, then  $R_s$  would be 0, and the index  
397 would be 1. Conversely, if the repulsion all came from cross-fixation interactions, then  $R_d$  and  
398  $R_s$  would be identical, and the index would be 0. The results are shown in Fig. 6b. We found  
399 that as expected, the contribution of the cross-trial adaptation to the repulsion was small even for  
400  $n = 1$  and disappeared for  $n = 4$ . The sum of the indices across  $n$  is around 0.2, well below 1,  
401 and thus cannot account for the observed repulsion. Second, we investigated the possibility that  
402 different  $n$ -back adaptation effects might sum superlinearly to explain the repulsion. We therefore  
403 determined the cumulative  $n$ -back adaptation effect directly, instead of summing the separate  $n$ -  
404 back effects. To this end, we defined the "same" and "different" sets according to whether the  
405 stimulus orientation of a trial were identical to, or different from, those of all  $n$  previous trials (which  
406 had to have the same orientation). The results in Fig. 6c show that the  $n$ -back cumulative effect had  
407 the index saturated around 0.25 for  $n = 3$ , again well below 1. The error bar grew with  $n$  because  
408 when  $n$  increased by 1, the available data was halved. We conclude that traditional adaptation  
409 aftereffects across trials at the same site cannot explain the repulsion in the 2-line condition.

#### 410 **The first and second reports in a trial showed similar repulsion**

411 Ding et al. (2017) presented two lines in a trial sequentially (and subjects reported them sequen-  
412 tially); this allowed them to measure both the forward aftereffect (how much the first line repelled  
413 the second line) and the backward aftereffect (how much the second line repelled the first line).  
414 They found that the two aftereffects were similar for a given subject. As they noted, this result  
415 contradicts standard adaptation theories whose sequential considerations of sensory responses  
416 predict only the forward aftereffect, and prompted them to propose high-to-low-level decoding in  
417 working memory. In the current study, we presented two lines in a trial simultaneously so the  
418 forward and backward aftereffects were not defined. Nevertheless, subjects had to report the two  
419 lines sequentially, and we analyzed whether the first and second reports of a line were similar or  
420 not. For both the 2-line and 2-line-interrupt conditions, we calculated the means of the first and  
421 second reports for the 49° line separately, and did the same for the 54° line. Using the means  
422 of the 49° and 54° lines of the 1-line condition as the baselines, we determined the repulsion  
423 values for each line when it was reported first and second. The results (Fig. 7) indicate that the

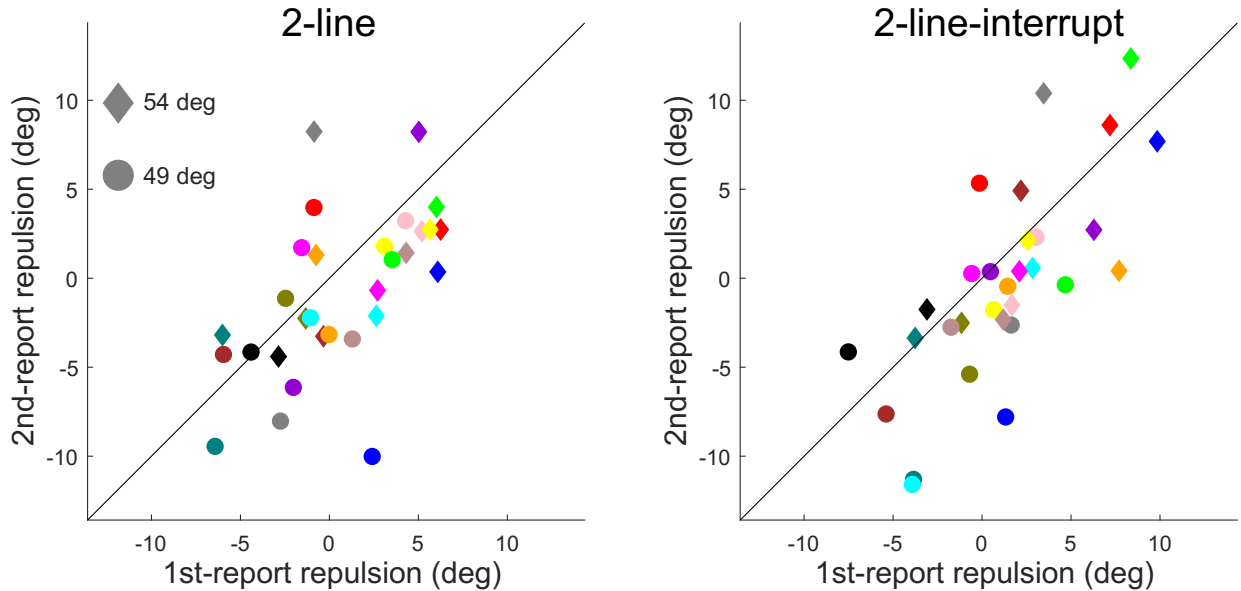


Figure 7: *First and second reports showed similar repulsion.* The left and right panels are for the 2-line and 2-line-interrupt conditions, respectively. In each panel, the second-report repulsion is plotted against the first-report repulsion across subjects. Each subject had two data points, one for the 49° line (round dot) and the other for the 54° line (diamond).

424 first and second reports showed similar repulsion, analogous to the similar backward and forward  
 425 aftereffects in Ding et al. (2017).

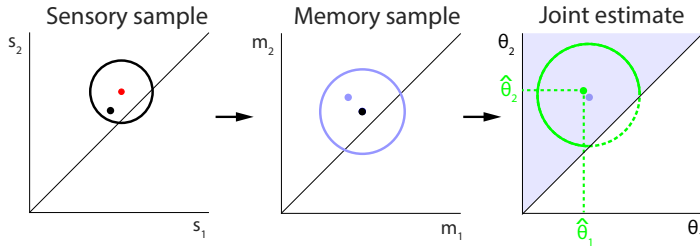
#### 426 **High-to-low-level Bayesian decoding explains the data from both report methods**

427 The cross-fixation interactions of orientations established above, in the form of repulsion and corre-  
 428 lation, cannot be explained by the low-to-high-level decoding scheme (Figs. 2-5). We thus adopted  
 429 Ding et al. (2017)'s high-to-low-level decoding scheme to account for the data. The main hypoth-  
 430 esis is that in a 2-line trial, subjects (implicitly) judged the lines' ordinal relationship and used this  
 431 higher-level information to constrain the decoding of the lower-level, absolute orientations of the  
 432 lines (Ding et al., 2017). To explain the differences between the two report methods, we applied  
 433 the scheme twice to take into account the interruption in the second report method, as detailed  
 434 below.

435 We started with the 1-line condition; we simply assumed that subjects made a noisy sensory  
 436 measurement of the stimulus line's orientation in a trial. Then the sensory sample was corrupted by  
 437 memory noise to produce a memory sample. We assumed both the sensory and memory noises  
 438 are Gaussian. With a uniform prior on orientation, the posterior was the same as the likelihood  
 439 function which was a Gaussian around the memory sample. Consequently, the decoded estimate

**a**

Model for 2-line condition

**b**

Model for 2-line-interrupt condition

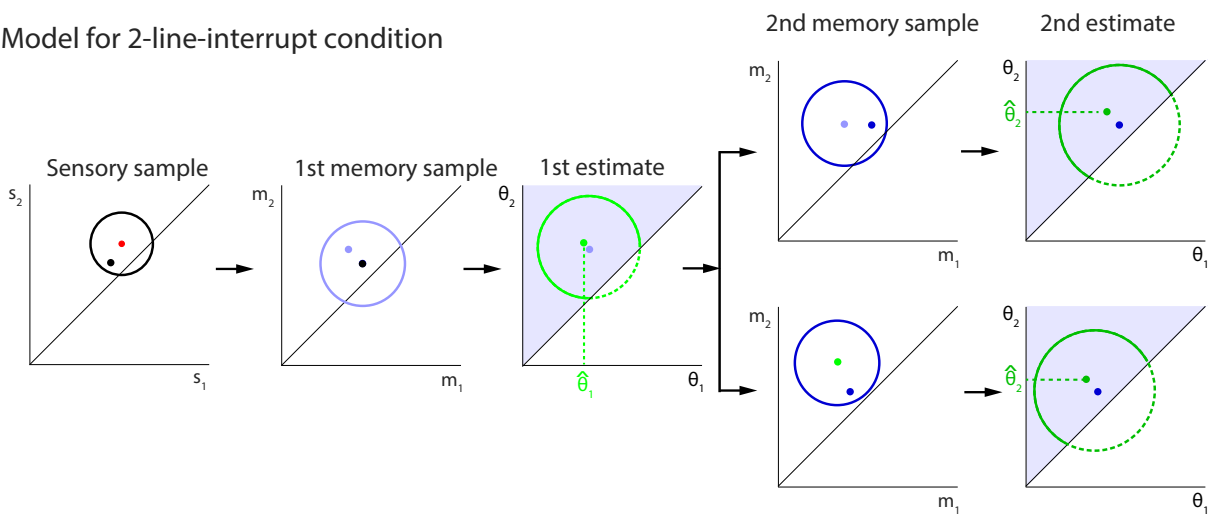


Figure 8: *High-to-low-level Bayesian decoding scheme*. (a) Model for the 2-line condition. First panel: a sensory sample (black dot) is drawn from the sensory distribution of the two lines (black circle) centered on the stimulus orientations (red dot). Second panel: a memory sample (blue dot) is drawn from the memory distribution (blue circle) centered on the sensory sample (black dot). Third panel: The posterior distribution (solid green arc above diagonal) is obtained by multiplying the likelihood function (green circle) centered on the memory sample (blue dot) and a Bayesian prior (shaded step function along the diagonal) from the ordinal judgment. The posterior mean is the decoded estimate of the two orientations (green dot). (b) Model for the 2-line-interrupt condition. It is similar to the 2-line model above except that the memory decoding process is repeated, one before and the other after the interruption, and each process reports only one of the two estimated orientations. The second decoding process is represented by the darker blue and green colors. The distribution (dark blue circle) for the second memory sample (dark blue dot) can be centered either on the first memory sample (top row) or on the first estimate (bottom row), resulting in two versions of the model.

440 was identical to the memory sample. These estimates were used in the above simulations of the  
441 low-to-high-level decoder that used the 1-line data to predict the 2-line data. As noted above, the  
442 low-to-high-level predictions did not match the data.

443 In the high-to-low-level decoding model for the 2-line condition (Fig. 8a), we also started with  
444 drawing sensory and memory samples (black and light blue dots, respectively) for a trial according  
445 to the sensory and memory noise distributions (black and light blue circles, respectively). The key  
446 difference was that the prior was not uniform but determined by subjects' ordinal judgment based  
447 on the sensory measurements. For instance, if the ordinal judgment was that the 54° orientation  
448 was greater than the 49° orientation, then the prior was non-zero only above the diagonal line in  
449 the joint space (the shaded region in the last panel of Fig. 8a). As a result, combining the likeli-  
450 hood function (green circle) and this step-function prior led to a posterior distribution (solid green  
451 arc) whose center of mass (green dot), the decoded estimate, was shifted away from the diag-  
452 onal. Note that here we modeled sensory and memory noises separately instead of grouping them  
453 together as in (Ding et al., 2017). The reason was that here the stimulus lines were presented  
454 simultaneously so that subjects could make ordinal judgments based solely on the sensory ev-  
455 idence. As explained in Ding et al. (2017), the binary, ordinal judgments were assumed to be  
456 resistant to memory noise. In contrast, the continuous, absolute orientations of the lines were  
457 degraded by the memory noise.

458 For the 2-line-interrupt condition, we used the same high-to-low-level decoding scheme as for  
459 the 2-line condition but we assumed that there were two decoding processes (Fig. 8b), one before,  
460 and the other after, the interruption (the disappearance of the marker line). Specifically, the first  
461 decoding process was identical to that for the 2-line condition. However, although both absolute  
462 orientations were decoded, only the left orientation was reported before the interruption. With  
463 the redrawing of the marker line after the interruption, we assumed a repeat of the decoding  
464 process but this time only the right orientation was reported. The second memory sample could  
465 be based on the first memory sample but further corrupted by the memory noise (Fig. 8b, first  
466 row). Alternatively, it could be based on the first estimate, also further corrupted by the memory  
467 noise (Fig. 8b, second row). We considered both versions of the model. We let the additional  
468 memory noise for the second decoding be the same as that for the first decoding because the  
469 reaction times of the two reports were similar in the 2-line-interrupt condition (see Supplementary  
470 Fig. S4).

471 The free parameters were the standard deviations for the sensory and memory noises (see  
472 Methods). We first jointly fit the parameters by maximizing the likelihood of the data of the 1-line  
473 and 2-line conditions. The resulting model matched the data well (Fig. 9, the first two columns).  
474 Notably, the model reproduced the characteristic repulsion, correlation, and the bimodal pattern in  
475 the 2-line joint distribution (Fig. 9, second column). We then used the fit parameters to generate

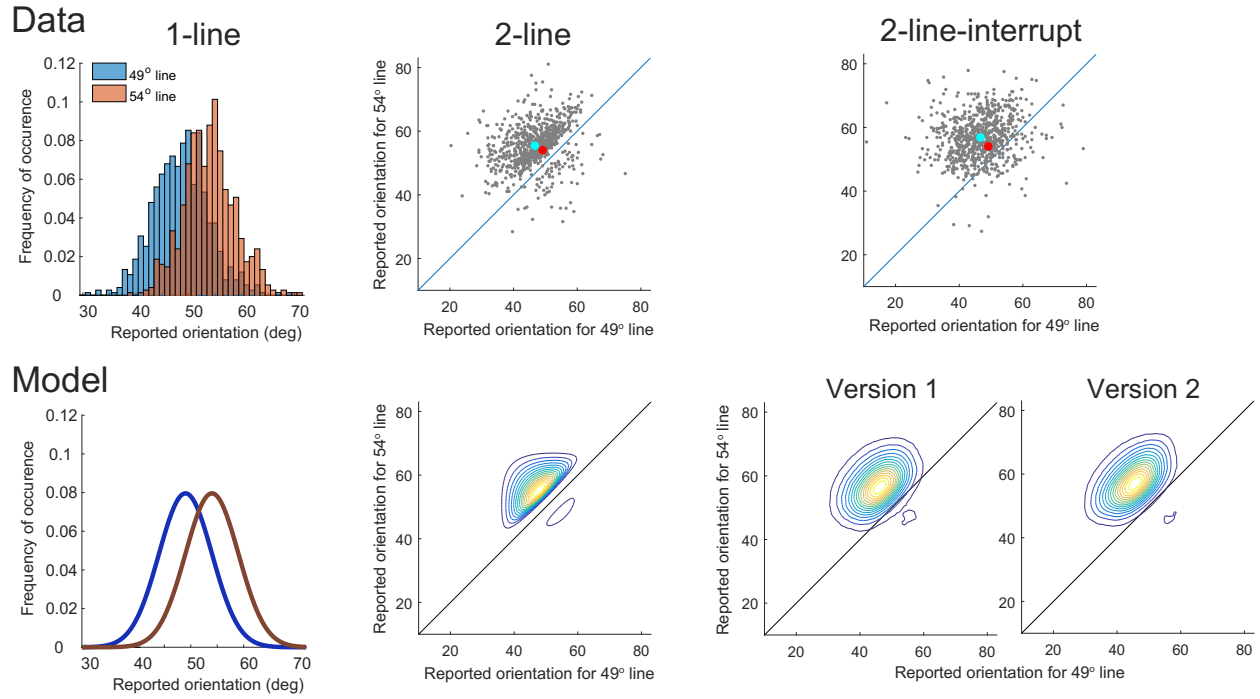


Figure 9: *Model fit of the 1-line and 2-line data, and prediction of the 2-line-interrupt data.* The first row shows the data (pooled over all subjects) and the second row shows the model fit or prediction. The first column shows the absolute distributions of the 1-line condition. The second column shows the joint distribution of the 2-line condition. The third column shows the joint distribution of the 2-line-interrupt condition, with two different model versions.

476 parameter-free predictions for the 2-line-interrupt condition. Both model versions for the 2-line-  
 477 interrupt conditions (Fig. 9, last column) fit the data similarly well. We also compared the measured  
 478 and the modeled difference distributions in Fig. 10, again showing good agreements.

## 479 Discussion

480 In this study, we tested a prediction of Ding et al. (2017)'s theory positing that visual decoding often  
 481 occurs in working memory where it progresses from high- to low-level features, with higher-level  
 482 features, which are more invariant, reliable, and behaviorally relevant, constraining the decod-  
 483 ing of lower-level features. Since the high-to-low-level constraints introduce interactions between  
 484 lower-level features, the theory predicts that low-level features that are traditionally considered as  
 485 independent may interact with each other when they are decoded in working memory.

486 In our experiment, the lower- and higher-level features were the absolute orientations of two lines  
 487 (on opposite sides of the fixation) and their ordinal relationship, respectively. Their *encoding* likely  
 488 follows the standard low-to-high-level hierarchy of sensory responses (Hubel and Wiesel, 1968;

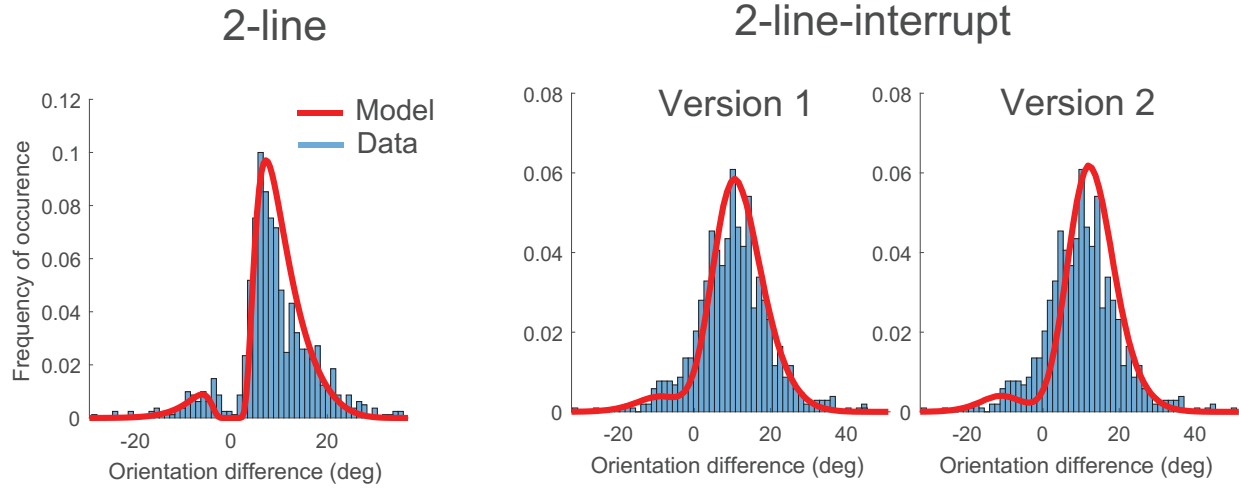


Figure 10: *Model fit and prediction of the difference distributions*. The first panel shows the fit (red curve) to the 2-line difference distribution (blue histogram). The last two panels shows the two model versions' predictions (red curves) of the 2-line-interrupt data (blue histogram).

489 Riesenhuber and Poggio, 1999; Anzai et al., 2007). The traditional view is that their *decoding*  
 490 follows the same hierarchy, and the absolute orientations are decoded in an early visual area with  
 491 small receptive fields and thus should be mutually independent. In contrast, according to Ding et al.  
 492 (2017), the encoded absolute orientations and their ordinal relationship enter working memory  
 493 after the disappearance of the stimuli. During the delay before the reports, the stored binary  
 494 ordinal relationship is noise resistant whereas the continuous absolute orientations are corrupted  
 495 by noise over time. By the report time, the brain decodes the reliable ordinal relationship first, and  
 496 uses it to constrain the decoding of the unreliable absolute orientations, producing interactions  
 497 between the absolute orientations. Using an eye-tracker to ensure fixation, we indeed found the  
 498 predicted cross-fixation interactions of the orientations in the form of repulsion and correlation.  
 499 Control experiments and analyses ruled out alternative explanations such as reporting-method  
 500 bias and cross-trial adaptation aftereffects on the same side of the fixation. Finally, we showed  
 501 that Ding et al. (2017)'s retrospective Bayesian decoding model well fit the 2-line data, and without  
 502 new free parameters, predicted the 2-line-interrupt data. Unlike many Bayesian models that adjust  
 503 priors to fit the data, in our simulations, the prior is a step function fully determined by the ordinal  
 504 judgment and only the likelihood function has free parameters.

505 We used a continuous and an interrupt report method for the 2-line and 2-line-interrupt conditions,  
 506 respectively. The continuous report method was nearly identical that of Ding et al. (2017),  
 507 and the 2-line data here resembled those of Ding et al. (2017) showing repulsion and correlation  
 508 between the two reported orientations in a trial. The interrupt report method was nearly iden-  
 509 tical to that of Bae and Luck (2017), and our 2-line-interrupt data were similar to those of Bae  
 510 and Luck (2017), showing repulsion but reduced correlation. Importantly, however, we placed the

511 two orientations on opposite sides of the fixation whereas both Ding et al. (2017) and Bae and  
512 Luck (2017) placed them (successively) at the fixation. Therefore, the current study demonstrated  
513 cross-fixation interactions of orientations whereas the two previous studies were not designed to  
514 do so. On the other hand, the three studies collectively indicate that when two orientations are  
515 both task relevant and decoded in working memory, they interact with each other regardless of  
516 whether they appear on the same or different retinal locations. In addition to retinal locations,  
517 these studies also differ in stimulus shape, size, eccentricity, and duration, the magnitude of orien-  
518 tation difference, and simultaneous vs. sequential presentations. The fact that they still produced  
519 similar results suggests that stimulus interactions in working memory are a robust phenomenon.

520 Both frontal/parietal areas and various sensory cortices have been implicated in working mem-  
521 ory (Pasternak and Greenlee, 2005). Since working memory does not necessarily require sus-  
522 tained neuronal firing after stimulus disappearance (Mongillo et al., 2008), it could in principle re-  
523 side even in low-level sensory areas. However, the working memory area for orientation decoding  
524 in our experiments is likely a high-level area that does not maintain fine retinotopy but instead, let  
525 relevant features from different locations affect each other. A related finding is the transfer of per-  
526 ceptual learning between well-separated retinal locations under certain training procedures (Xiao  
527 et al., 2008). For example, contrast training at one location transferred to another location that  
528 only received orientation training. Although there are key differences between short-term working  
529 memory and long-term perceptual learning, these studies, and that of Ding et al. (2017), sug-  
530 gest that perceptual decoding of low-level features could occur in high-level brain areas where the  
531 binding or integration of the features may produce various interactions among them across space  
532 and time. Alternatively, low-level features might be stored retinotopically in low-level sensory ar-  
533 eas which are modulated by high-level feedback connections to produce perceptual interactions  
534 (Pasternak and Greenlee, 2005). In either case, high-level processing must be involved in the  
535 decoding of low-level features.

536 Sensory processing and working memory are often treated as separate topics in the litera-  
537 ture. Our theory, however, explicitly integrates them by proposing that decoding of perceptual  
538 judgments may happen in working memory. It is this integration that provides a key reason that  
539 decoding should proceed from high- to low-level features (Ding et al., 2017), which then leads to  
540 our prediction of cross-fixation interactions of orientations (see Introduction). Since sensory pro-  
541 cessing includes both encoding and decoding, we consider decoding in working memory as part  
542 of sensory processing. Alternatively, one may argue that working memory should not be included  
543 in sensory processing. Accordingly, our framework becomes the following: sensory processing  
544 proceeds from low- to high-level features, and high-to-low-level decoding of perceptual judgments  
545 in working memory should just be viewed as a memory process, not part of the sensory process.  
546 We note that this is mostly an issue of definition that does not change our reasoning on why de-

547 coding in working memory should proceed from high- to low-level features or how higher-level  
548 features should constrain the decoding of lower-level features.

549 Binary ordinal judgments could also be viewed as perceptual decisions. So an equivalent inter-  
550 pretation of our model is that the perceptual decision on the ordinal relationship provides a prior  
551 to constrain the decoding of the absolute orientations. What is important, however, is not the  
552 different choices of terminology, but the common theme that the higher-level ordinal relationship  
553 between two lines affects the decoding of the lower-level absolute orientations of the individual  
554 lines. Therefore, the decision interpretation is consistent with our high-to-low-level decoding hier-  
555 archy. On the other hand, without the consideration of different noise tolerance of low- vs. high-  
556 level features in working memory, the decision interpretation alone misses a key reason of why the  
557 high-to-low-level decoding scheme is desirable (Ding et al., 2017). Also note that the binary, ordi-  
558 nal decision was not a separate task imposed on the subjects. For the 2-line-interrupt condition,  
559 the ordinal decision was not even implicitly required. Our study is therefore different from typical  
560 task-dependence studies where the tasks in question are usually required. Additionally, unlike our  
561 theory, task dependence alone does not provide a reason on why decoding should proceed from  
562 high- to low-level features in working memory or how higher-level features should constrain the  
563 decoding of lower-level features.

564 As noted above, according to Ding et al. (2017), interactions between lower-level features in  
565 working memory stems from higher-level constraints on lower-level decoding. In our experiments,  
566 the lower-level features were the individual, absolute orientations of the two lines, and the higher-  
567 level feature was their ordinal relationship. For the continuous report method (2-line condition),  
568 subjects implicitly indicated their ordinal choice when rotating the marker line continuously from  
569 the first report to the second report of the absolute orientations. In contrast, for the interrupt re-  
570 port method (2-line-interrupt condition), because the marker line disappeared after the first report,  
571 subjects could not use the continuous rotation to indicate their ordinal choice. The fact the the  
572 2-line-interrupt data can be explained by the same high-to-low-level decoding scheme (applied  
573 twice but without new free parameters) suggests that the ordinal relationship was still decoded  
574 first, which then constrained the absolute decoding, even when its reporting was not required. The  
575 reason, we believe, is that the ordinal relationship is more invariant against viewing conditions,  
576 more reliable against memory noise, and more behaviorally useful, than the absolute orienta-  
577 tions so that the brain may automatically prioritize its decoding. When the ordinal relationship is  
578 decoded correctly, it can then help improve the decoding of less reliable, absolute orientations  
579 through the high-to-low-level constraint (Ding et al., 2017). High-to-low-level decoding in noisy  
580 working memory could be a general principle for understanding perception.

581 **Acknowledgment**

582 Supported by NSF grant 1754211, AFOSR grant FA9550-15-1-0439, and Irving Weinstein Foun-  
583 dation Inc.

584 **References**

585 Peggy Seriès, Alan A Stocker, and Eero P Simoncelli. Is the homunculus “aware” of sensory  
586 adaptation? *Neural Computation*, 21(12):3271–3304, 2009.

587 Li Zhaoping. *Understanding vision: theory, models, and data*. Oxford University Press, USA, 2014.

588 Daniel J Felleman and DC Essen Van. Distributed hierarchical processing in the primate cerebral  
589 cortex. *Cerebral cortex*, 1(1):1–47, 1991.

590 James J DiCarlo, Davide Zoccolan, and Nicole C Rust. How does the brain solve visual object  
591 recognition? *Neuron*, 73(3):415–434, 2012.

592 Daniel LK Yamins and James J DiCarlo. Using goal-driven deep learning models to understand  
593 sensory cortex. *Nature neuroscience*, 19(3):356, 2016.

594 Daniel LK Yamins, Ha Hong, Charles F Cadieu, Ethan A Solomon, Darren Seibert, and James J  
595 DiCarlo. Performance-optimized hierarchical models predict neural responses in higher visual  
596 cortex. *Proceedings of the National Academy of Sciences*, 111(23):8619–8624, 2014.

597 Maximilian Riesenhuber and Tomaso Poggio. Hierarchical models of object recognition in cortex.  
598 *Nature neuroscience*, 2(11):1019, 1999.

599 Thomas Serre, Aude Oliva, and Tomaso Poggio. A feedforward architecture accounts for rapid  
600 categorization. *Proceedings of the national academy of sciences*, 104(15):6424–6429, 2007.

601 Radoslaw Martin Cichy, Aditya Khosla, Dimitrios Pantazis, Antonio Torralba, and Aude Oliva. Com-  
602 parison of deep neural networks to spatio-temporal cortical dynamics of human visual object  
603 recognition reveals hierarchical correspondence. *Scientific reports*, 6:27755, 2016.

604 David Marvin Green, John A Swets, et al. *Signal detection theory and psychophysics*, volume 1.  
605 Wiley New York, 1966.

606 MA Paradiso. A theory for the use of visual orientation information which exploits the columnar  
607 structure of striate cortex. *Biological cybernetics*, 58(1):35–49, 1988.

608 H Sebastian Seung and Haim Sompolinsky. Simple models for reading neuronal population codes.  
609 *Proceedings of the National Academy of Sciences*, 90(22):10749–10753, 1993.

610 Arnulf BA Graf, Adam Kohn, Mehrdad Jazayeri, and J Anthony Movshon. Decoding the activity of  
611 neuronal populations in macaque primary visual cortex. *Nature neuroscience*, 14(2):239, 2011.

612 Andrew F Teich and Ning Qian. Learning and adaptation in a recurrent model of v1 orientation  
613 selectivity. *Journal of Neurophysiology*, 89(4):2086–2100, 2003.

614 Stephanie Ding, Christopher J Cueva, Misha Tsodyks, and Ning Qian. Visual perception as  
615 retrospective bayesian decoding from high-to low-level features. *Proceedings of the National  
616 Academy of Sciences*, 114(43):E9115–E9124, 2017.

617 John J Hopfield. Neurons with graded response have collective computational properties like  
618 those of two-state neurons. *Proceedings of the national academy of sciences*, 81(10):3088–  
619 3092, 1984.

620 Albert Compte, Nicolas Brunel, Patricia S Goldman-Rakic, and Xiao-Jing Wang. Synaptic mech-  
621 anisms and network dynamics underlying spatial working memory in a cortical network model.  
622 *Cerebral cortex*, 10(9):910–923, 2000.

623 Vladimir Itskov, David Hansel, and Misha Tsodyks. Short-term facilitation may stabilize parametric  
624 working memory trace. *Frontiers in computational neuroscience*, 5:40, 2011.

625 James J Gibson and Minnie Radner. Adaptation, after-effect and contrast in the perception of tilted  
626 lines. i. quantitative studies. *Journal of experimental psychology*, 20(5):453, 1937.

627 Xin Meng, Pietro Mazzoni, and Ning Qian. Cross-fixation transfer of motion aftereffects with ex-  
628 pansion motion. *Vision research*, 46(21):3681–3689, 2006.

629 Hong Xu, Peter Dayan, Richard M Lipkin, and Ning Qian. Adaptation across the cortical hier-  
630 archy: Low-level curve adaptation affects high-level facial-expression judgments. *Journal of  
631 Neuroscience*, 28(13):3374–3383, 2008.

632 Helen C Beh, Peter M Wenderoth, and AT Purcell. The angular function of a rod-and-frame illusion.  
633 *Perception & Psychophysics*, 9(4):353–355, 1971.

634 L. Luu and A.A. Stocker. Post-decision biases reveal a self-consistency principle in perceptual  
635 inference. *eLife*, In press. 2018.

636 Alan A Stocker and Eero P Simoncelli. A bayesian model of conditioned perception. In *Advances  
637 in neural information processing systems*, pages 1409–1416, 2008.

638 Cheng Qiu, Long Luu, and Alan A Stocker. Benefits of commitment in hierarchical inference.  
639 *Psychological review*, 127(4):622, 2020.

640 Matthias Fritzsche and Floris P de Lange. Reference repulsion is not a perceptual illusion. *Cogni-  
641 tion*, 184:107–118, 2019.

642 M. Jazayeri and J.A. Movshon. A new perceptual illusion reveals mechanisms of sensory decod-  
643 ing. *Nature*, 446:912ff, April 2007.

644 E. Zamboni, T. Ledgeway, P.V. McGraw, and D. Schluppeck. Do perceptual biases emerge early  
645 or late in visual processing? decision-biases in motion perception. *Proc. of Royal Society of*  
646 *London B*, 283(1833), 2016. doi: 10.1098/rspb.2016.0263.

647 Z. Z. Bronfman, N. Brezis, R. Moran, K. Tsetsos, T. Donner, and M. Usher. Decisions reduce  
648 sensitivity to subsequent information. *Proceedings of the Royal Society of London B: Biological*  
649 *Sciences*, 282(1810), 2015. doi: 10.1098/rspb.2015.0228.

650 Bharath Chandra Talluri, Anne E Urai, Konstantinos Tsetsos, Marius Usher, and Tobias H Don-  
651 ner. Confirmation bias through selective overweighting of choice-consistent evidence. *Current*  
652 *Biology*, 28(19):3128–3135, 2018.

653 Gi-Yeul Bae and Steven J Luck. Interactions between visual working memory representations.  
654 *Attention, Perception, & Psychophysics*, 79(8):2376–2395, 2017.

655 Qinglin Li, Andrew Isaac Meso, Nikos K Logothetis, and Georgios A Keliris. Scene regularity  
656 interacts with individual biases to modulate perceptual stability. *Frontiers in neuroscience*, 13,  
657 2019.

658 David Navon. Forest before trees: The precedence of global features in visual perception. *Cogni-  
659 tive psychology*, 9(3):353–383, 1977.

660 Lin Chen. Topological structure in visual perception. *Science*, 218(4573):699–700, 1982.

661 Merav Ahissar and Shaul Hochstein. The reverse hierarchy theory of visual perceptual learning.  
662 *Trends in cognitive sciences*, 8(10):457–464, 2004.

663 Aude Oliva and Antonio Torralba. Building the gist of a scene: The role of global image features  
664 in recognition. *Progress in brain research*, 155:23–36, 2006.

665 Richard C Atkinson and Richard M Shiffrin. Human memory: A proposed system and its control  
666 processes. In *Psychology of learning and motivation*, volume 2, pages 89–195. Elsevier, 1968.

667 Gail A Carpenter and Stephen Grossberg. A massively parallel architecture for a self-organizing  
668 neural pattern recognition machine. *Computer vision, graphics, and image processing*, 37(1):  
669 54–115, 1987.

670 Shimon Ullman. Sequence seeking and counter streams: a computational model for bidirectional  
671 information flow in the visual cortex. *Cerebral cortex*, 5(1):1–11, 1995.

672 Tai Sing Lee and David Mumford. Hierarchical bayesian inference in the visual cortex. *JOSA A*,  
673 20(7):1434–1448, 2003.

674 Long Luu, Mingsha Zhang, Misha Tsodyks, and Ning Qian. Cross-fixation interactions of orien-  
675 tations suggest that orientation decoding occurs in a high-level area of visual working memory.  
676 *Journal of Vision*, 20(11):216–216, 2020.

677 David H Brainard. The psychophysics toolbox. *Spatial vision*, 10(4):433–436, 1997.

678 Jason Fischer and David Whitney. Serial dependence in visual perception. *Nature neuroscience*,  
679 17(5):738–743, 2014.

680 David H Hubel and Torsten N Wiesel. Receptive fields and functional architecture of monkey  
681 striate cortex. *The Journal of physiology*, 195(1):215–243, 1968.

682 Akiyuki Anzai, Xinmiao Peng, and David C Van Essen. Neurons in monkey visual area v2 encode  
683 combinations of orientations. *Nature neuroscience*, 10(10):1313–1321, 2007.

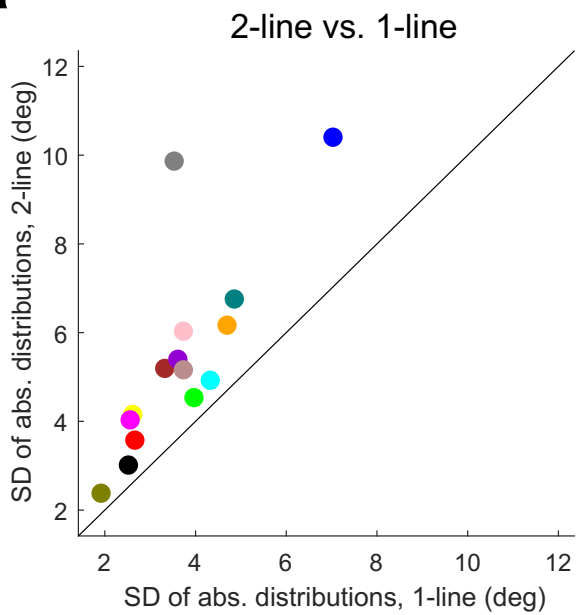
684 Tatiana Pasternak and Mark W Greenlee. Working memory in primate sensory systems. *Nature  
685 Reviews Neuroscience*, 6(2):97–107, 2005.

686 Gianluigi Mongillo, Omri Barak, and Misha Tsodyks. Synaptic theory of working memory. *Science*,  
687 319(5869):1543–1546, 2008.

688 Lu-Qi Xiao, Jun-Yun Zhang, Rui Wang, Stanley A Klein, Dennis M Levi, and Cong Yu. Com-  
689 plete transfer of perceptual learning across retinal locations enabled by double training. *Current  
690 Biology*, 18(24):1922–1926, 2008.

691 **Supplementary information**

**a**



**b**

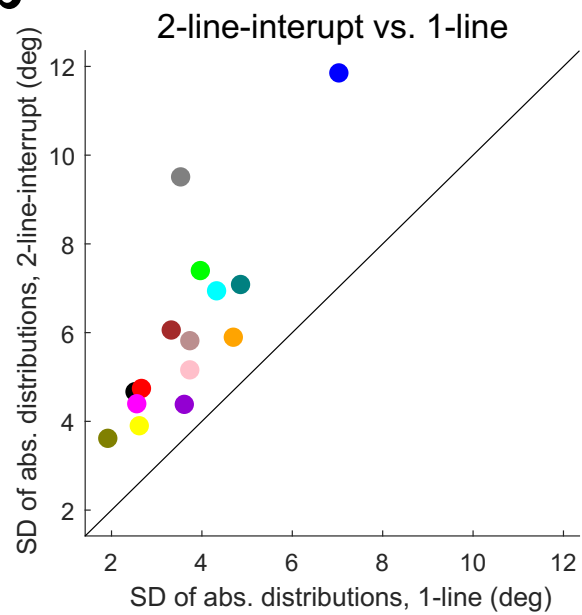


Figure S1: *More memory noise in the 2-line and 2-line-interrupt conditions than in the 1-line condition.* For each condition, the SD is the square root of a subject's mean of the variances for the  $49^\circ$  and  $54^\circ$  absolute distributions. (a) The 2-line condition vs. the 1-line condition. (b) The 2-line-interrupt condition vs. 1-line condition.

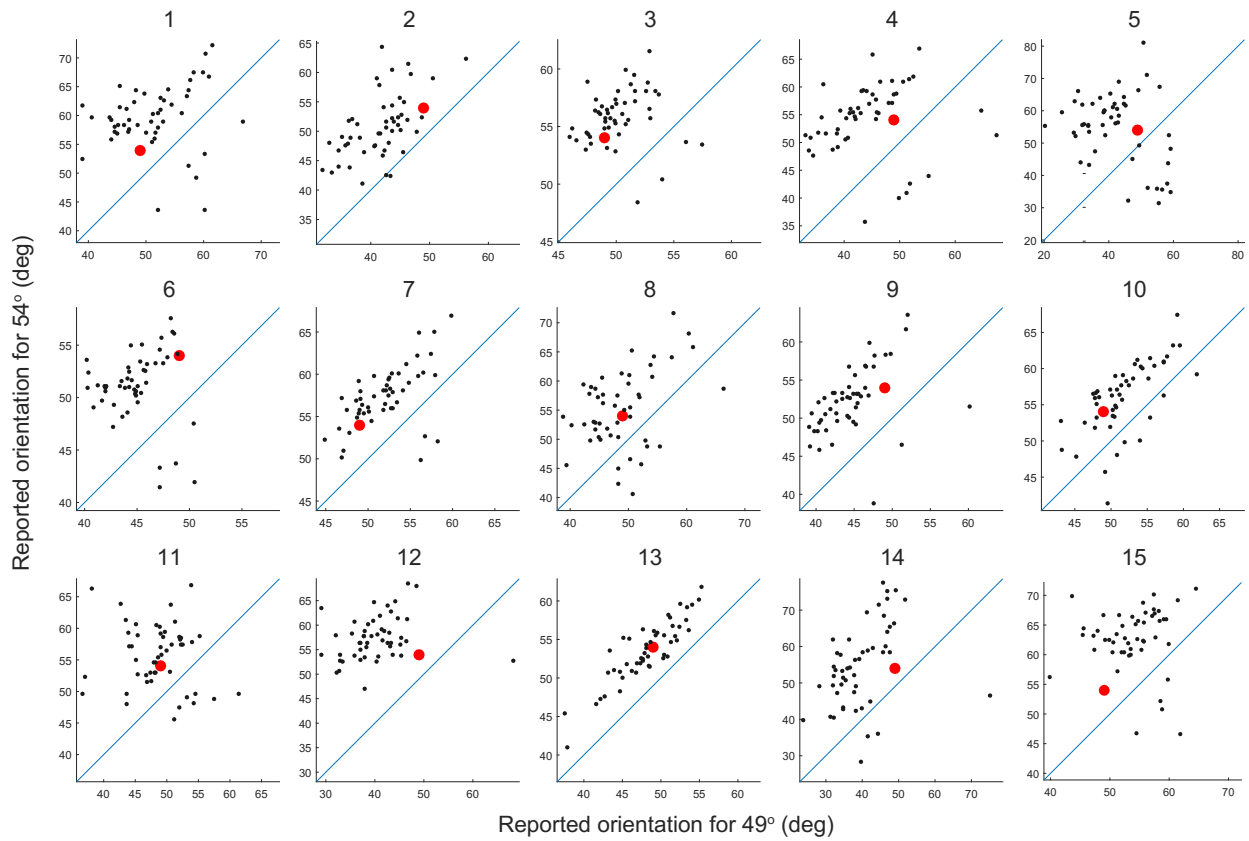


Figure S2: *Joint distributions of individual subjects in the 2-line condition.*

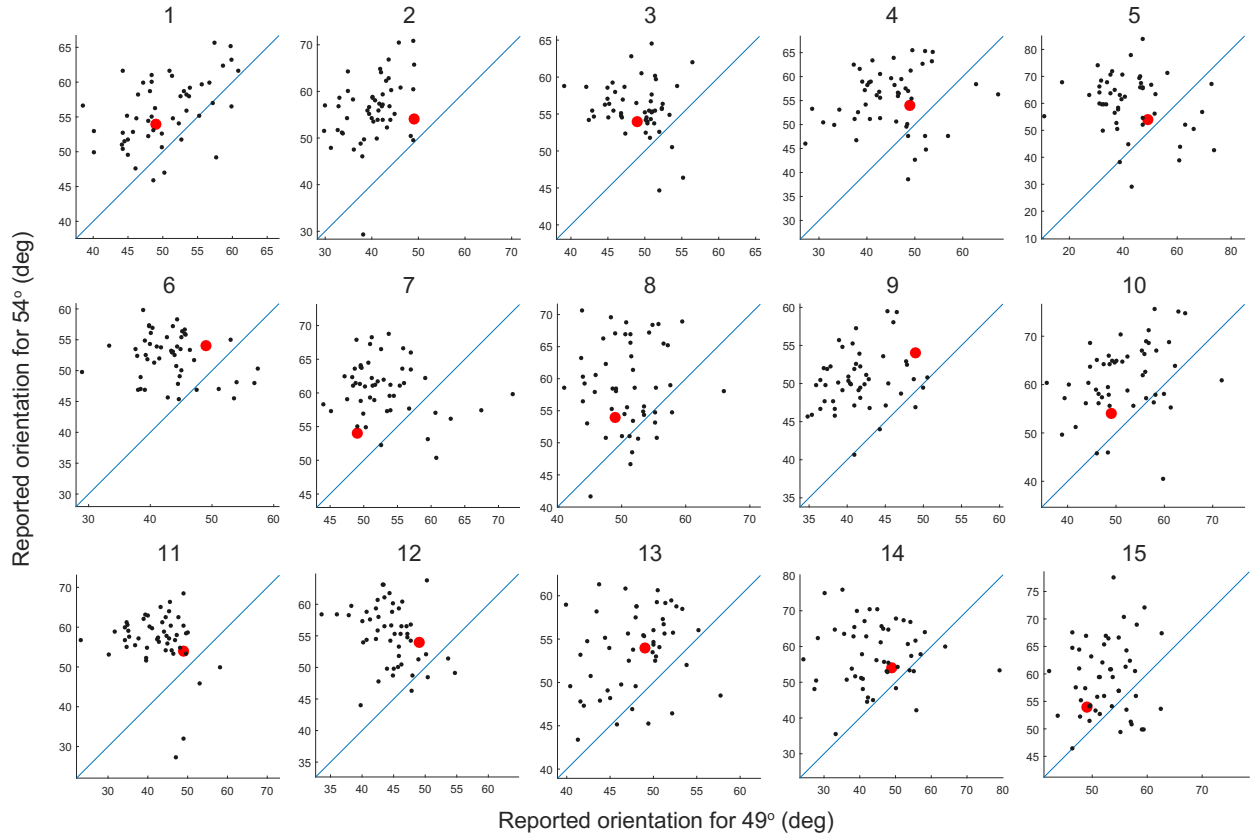


Figure S3: *Joint distributions of individual subjects in the 2-line-interrupt condition.*

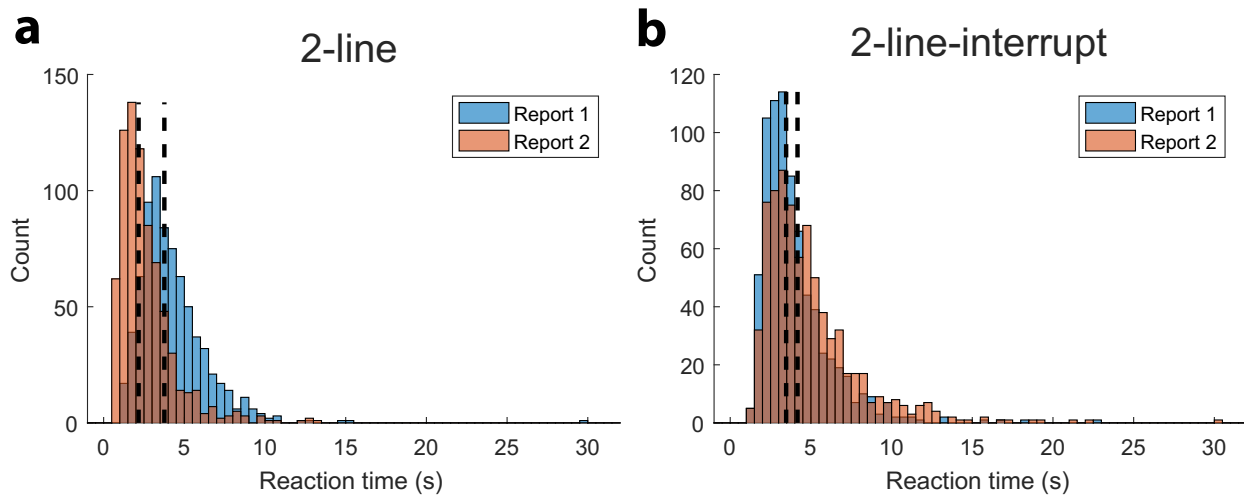


Figure S4: *Reaction time distributions in the 2-line (a) and 2-line-interrupt (b) conditions.* Data are pooled from all subjects. In each panel, the reaction time (RT) distributions for the first and second reports in a trial are shown in blue and orange, respectively. The vertical lines indicate the means. The mean RT difference between the two reports in a trial were 1.6 and -0.7 sec for the 2-line and 2-line-interrupt conditions, respectively.